RSC Advances

ROYAL SOCIETY OF CHEMISTRY

www.rsc.org/advances

DNAzyme Catalytic Beacons-based a label–free biosensor for copper using electrochemical impedance spectroscopy

Wenyong Hu[a,b*], Xiaobo Min[a,b*], Xinyu Li[a,b], Shengxiang Yang[a,b], Langbo Yi[a,b], Liyuan Chai[a,b]

[a] School of Metallurgy and Environment, Central South University, Changsha, 410083, China,

[b] National Engineering Research Center for Pollution Control of Heavy Metals, Changsha 410083, Hunan, PR China.

[*] Corresponding author: Tel.: +86 13762157065; Fax.: +86 0731 88710171

E–mail: huwenyong07@126.com (W.Y. Hu). mxb@csu.edu.cn (X. B. Min)

ABSTRACT

In this work, we developed a novel selective method for copper quantification based on gold nanoclusters (GNCs) and DNAzyme. The GNCs were used as sensing interface to immobilize with the DNAzyme capturing Cu^{2+} ions. The DNAzyme could be activated to cleave the substrate strand into two DNA fragments in the presence of Cu^{2+}, and produces changes in the interfacial properties of the electrode. The difference in the interfacial electron-transfer resistance is probed in the presence of the reversible redox couple $Fe(CN)_6^{3-/4-}$ as a marker using electrochemical impedance spectroscopy (EIS). And Randles equivalent circuit was employed to evaluate the EIS results. The charge transfer resistance (R_{CT}) value for the $Fe(CN)_6^{3-/4-}$ redox indicator was remarkably decline after hybridization with Cu^{2+}. The difference in R_{CT} values before and after hybridization with Cu^{2+} showed a linear relation with the concentration of the Cu^{2+} in a range of 0.1–400 nM, with a detection limit of 0.0725 nM (S/N=3). Furthermore, with the application of Cu^{2+} dependent DNAzyme, the proposed sensing system exhibited high selectivity. This biosensor demonstrated a promising potential for Cu^{2+} detection in real sample.

Keywords: Impedimetric sensor; Copper; Label–free; DNAzyme;

1. **Introduction**

Copper is used widely that can leak into the natural environment through various routes. Low concentration of copper is an essential nutrient. However, exposure to high level of copper can cause gastrointestinal disturbance even for a short period of time, while long term exposure causes liver or kidney damage[1, 2]. Therefore, the development of a sensitive, selective and comparatively inexpensive method for Cu^{2+} ion detection is of great significance. Traditional quantitative methods, for example, atomic absorption spectrometry (AAS)[3], and inductively coupled plasma mass spectroscopy (ICP/MS)[4], and etc, provide reliable and accurate results, but require expensive and sophisticated instrumentation and complicated sample pretreatment. Many electrochemical sensors such as voltammetric[5, 6] and electrochemiluminescence sensors[7, 8] are simple and relatively inexpensive, however, they suffer from low reproducibility and low selectivity. Therefore, Metal-biochemical and biophysical studies have attracted intense attention during the past few decades. Important insights have been gained regarding metal-DNAzymes sensors, the reason may be that DNAzymes–based biosensors have higher detection stability, sensitivity, and especially selectivity for a given metal reaction, on the contrary, insensitive to other metal ions even in complex environments, thus improving the potential application in real environment[9, 10].

Furthermore, it is a key technique for improving DNA sensing efficiencies that an effective immobilization platform for thiolated probe DNA and DNAzymes on the modified electrode. In recent years, various nanomaterials were employed as DNA immobilization substrates and recognition elements in biosensors. For example, Zhong and co–workers fabricated a simple but sensitive turn–off assay for Pb^{2+} detection with the 8–17DNAzyme based on single–walled carbon nanotubes (SWCNT)[11]. Tang et al.[9] used ordered mesoporous carbon–gold nanoparticle (OMC–GNPs) as the platform for electrochemical biosensors for the detection of Pb^{2+} concentration electrochemical impedance spectroscopy (EIS) with $Fe(CN)_6^{4-/3-}$ as the redox couple. These biosensors could increase the sensitivity and lower the detection limit for metal ions detection. In this study, gold nanoclusters (GNCs) were used as sensing interface to immobilize the DNA. In addition to its higher conductivity, excellent

structural continuity and general biocompatibility[12], GNCs also provides a natural platform for stable DNA immobilization because of the strong gold–sulfur (Au–S) covalent–type interactions, which might extend the using life and stability of the biosensor, and make the sensor assembly process easier. Though gold nanoclusters have been used in biosensors[12, 13], little attention has been paid to copper ion sensors based on DNAzyme-based biosensor.

Herein, a label–free biosensor with GNCs as a transducer platform with DNAzyme was developed for the detection of copper using EIS with selectivity and sensitivity. The interfacial properties (such as, electron transfer resistance and capacitance) of the electrode were investigated in the presence of a redox probe of $Fe(CN)_6^{3-/4-}$. In the presence of Cu^{2+}, the trans–acting catalytic beacon cleaves the sessile of the substrate into two fragments (Scheme 1), resulting in the remarkable decrease of interfacial charge–transfer resistance (R_{CT}) for the negatively charged redox probe at the electrochemical biosensor due to the enhanced electron transfer by GNCs. Taking advantage of the R_{CT} change, Cu^{2+} can be detected at the concentration as low as 0.0725 nM.

2. Experimental

2.1. Chemicals and Apparatus

Copper(II) chloride were purchased from Sigma–Aldrich (USA). $K_3Fe(CN)_6$, $K_4Fe(CN)_6$, sodium ascorbate and all other chemicals were of analytical grade and used as received. And all aqueous solutions were prepared using ultra–pure water (18 MΩ·cm, Milli–Q, Millipore). 50 mM tris–acetate buffer (pH 7.4) including 0.2 M NaCl and phosphate buffer saline (PBS, 0.1 M KH_2PO_4 and 0.1 M Na_2HPO_4), were used in this work. The DNA target–specific probes used for hybridization in the experiment were synthesized by Sangon (Shanghai, China) and purified using high–performance liquid chromatography. The sequences of the oligonucleotides include:

5'–HS–$(CH_2)_6$–GGTAAGCCTGGGCCTCTTTCTTTTTAAGAAAGAAC–3' (DNA S1)

5'– AGCTTCTTTCTAATACGGCTTACC–3' (DNA S2, a complementary substrate oligonucleotide of the DNAzyme)

CHI1230B A14535 electrochemical workstation (Chenhua Instrument, Shanghai, China) was used to carried out of the electrochemical impedance spectroscopy (EIS) measurement and cyclic voltammetric (CV) measurements. Besides, in this work, the three–electrode system includes in a saturated calomel electrode (SCE) as reference electrode, a Pt foil auxiliary electrode and a modified electrode as working electrode. Aglient7700x All the work was conducted at room temperature (25 °C) unless otherwise mentioned.

2.2. Sensor fabrication

Probe was activated by 2 mM TCEP (which is included to reduce disulfide bonded oligomers), and diluted by 50 mM tris–acetate buffer (pH 7.4). The bare glass carbon electrode (GCE) was polished in alumina slurry firstly, and then rinsed with deionized water. Finally, the electrode surface was treated using H_2SO_4 (0.5 M) with cyclic voltammetry scan (between 0 and 1.2 V at the scan rate of 50 mV s^{-1}) until a reproducible scan was obtained. After being dried, Au nanoprickle clusters were electrodeposited onto the GCE[14]. Electrodeposition was performed using chronoamperometry in 1% (w/w) $HAuCl_4$ solution containing perchloric acid at a potential of 0.18 V for 120 s. Following immersion in chloroform to dissolve the polycarbonate template, the obtained electrode was thoroughly rinsed with water.

Subsequently, the solution (7 μL DNA S1, 50 mM tris–acetate buffer (pH 7.4) was dropped onto the electrode surface for self–assembling through Au–S bonding for 12 h in 4 °C. The probes of this biosensor were hybridized as follows. 6–mercapto–1–hexanol (MCH) solution (400 μL) was used to immerse the modified electrode with DNA S1 probes with 30 min to improve the stability and quality, to reduce nonspecific adsorption of DNA and to obtain a well aligned DNA monolayer. Subsequently, the modified electrode was soaked in the solution with DNA S2, and incubated at room temperature for 70 min to yield the final copper–DNAzyme assembly on the surface. Then, the electrode was immersed in buffer (50 mM Tris–acetate, 0.2 M NaCl, pH 7.4) for 10 min to reduce the nonspecific adsorption of DNA S2. various concentrations of target Cu^{2+} in the buffer (50 mM Tris–acetate, 0.2 M sodium ascorbate, pH 7.4) was then allowed to react with the DNA surface (50 min in a 40 °C water bath) to

obtain the maximum cleavage of substrate strand on the modified electrode. Then the electrode was removed from the buffer, and allowed to cool down to room temperature within 1 hour.

Impedimetric detection

A CHI1230B A14535 electrochemical workstation was used, and all the measurements were carried out at room temperature with conventional three–electrode system. The modified electrode was treated with various concentrations of Cu^{2+} in buffers (50 mM tris–acetate, 0.2 M NaCl, pH 7.4) for 2 h. Subsequently, it was washed with tris–acetate buffer (pH=7.4). A conventional three–electrode system was used. Cyclic voltammograms (CVs) were performed in 0.1 M PBS (pH 7.0) containing 10 mM KCl and 5 mM $Fe(CN)_6^{3-/4-}$ (1:1). Besides, EIS was performed in 0.1 M PBS (pH 7.4) containing 5 mM $Fe(CN)_6^{3-/4-}$ (1:1) and 10 mM KCl in the frequency range from 0.1 Hz to 100 kHz with 5 mV as the amplitude at a polarization potential of 0.18 V. The data for condition optimization and the calibration curve were the average values of three measurements.

The impedance spectra were plotted in the form of complex plane diagram (-Z " vs. Z′), and fitted to a theoretical curve corresponding to the equivalent circuit by software of EIS Spectrum Analyser. And the interfacial resistance (R_{CT}) was obtained, which could be presumably due to changes in the film thickness for films of DNA S1 and DNA S2, which would increase the distance for electron transfer through the film and hence increase R_{CT}. Importantly, the trans–acting catalytic strand cleaved the sessile of the substrate into two fragments in the presence of Cu^{2+}, and the charge–transfer resistance R_{CT} was significantly reduced. The reason may be that the DNA S2 would introduce significant disorder into the solution, and the redox probe may penetrate the film to a larger extent, giving rise to a lower R_{CT}. In order to compare the results obtained from the electrodes used with or without Cu^{2+}, and to obtain relative signals. The ΔR_{CT} value was defined according to the following equations:

$$\Delta R_{CT} = R_{CT(DNAzyme)} - R_{CT(DNAzyme+Cu)}$$

where $R_{CT(DNAzyme+Cu)}$ was the electron transfer resistance value measured after incubation with copper; $R_{CT(DNAzyme)}$ was the electron transfer resistance value measured after DNAzyme immobilization on the electrode.

2.4 Analysis of environmental samples

As a further step, we attempted to provide the general applicability of this biosensor to practical samples. Four water samples were collected from Xiangjiang River, Hunan Province. After filtered through a 0.2 mM membrane to remove oils and other organic impurities, the samples were spiked with standard solutions of Cu^{2+} prior to measurement using the proposed method and ICP/MS (Aglient7700x, Aglient, USA).

3. Results and discussion

3.1. DNAzyme–based electrochemical sensor

As presented in Fig. 1, GNCs film was utilized as the platform for the immobilization of DNA and enhancing the transfer of electronics. Once in the presence of Cu^{2+}, the trans–acting catalytic strand cleaved the sessile phosphodiester of the substrate into two fragments, leading to the change of interfacial charge–transfer resistance of the electrodes towards the $Fe(CN)_6^{4-/3-}$ redox couple. As seen in Fig.1, after hybridization with probes, the impedance is relatively high, and in the presence of Cu^{2+}, the impedance shifted back. The reason might be ascribed to easier electron transfer between GCE surface and $Fe(CN)_6^{3-/4-}$ with Cu^{2+}. Thus the electron transfer of the whole system could be accelerated. In fact, the changes of the charge transfer resistance (ΔR_{CT}) of DNA films in the presence and absence of the metal ion were different and dependent on the concentration of the given metal ion. The result also coincided with the presumptive mechanism on the Cu^{2+} induced conformational change of the hybridization probes, thus enhanced the electron transfer of $Fe(CN)_6^{4-/3-}$ redox couple. The various conformational characteristics and charge of DNA on the surface result in different charge–transfer resistances for the redox indicator ions. Based on this principle, the interaction between DNA and Cu^{2+} led to the decrease of R_{CT}, and ΔR_{CT} was related to the concentration of Cu^{2+}.

"Here Fig. 1"

3.2. Characterization of electrode and optimization of the variables of experimental conditions

As seen in Fig. S-1A, the gold nanoparticles were electrodeposited onto the surface of GCE, and protuberant clusters grew along the pores of the polycarbonate template. The mean diameter of the Au nanoclusters was around 100 nm. Besides, to test the performance of the modified electrode, CV was carried out in phosphate buffer (containing 5 mM $Fe(CN)_6^{3-/4-}$ (1:1) and 10 mM KCl, pH 7.4). As seen in Fig. S-1B, the peak current of the redox probe was increased significantly after the immobilization of GNCs on the GCE. These cyclic voltammograms also proved that the electrode had a good current response capability. Correspondingly, EIS showed that the impedance of the GNCs/GCE and bare GCE in phosphate buffer. An almost straight line was observed with GNCs assembled, however, an obvious increase in the interfacial resistance was observed from the GCE (Fig. S-1C), which indicated that the introduction of GNCs could enhance the electron transfer kinetics to a large extent. What's more, the electron transfer ability of the modified electrode reflected by EIS was in accordance with the current density response reflected by CV.

The experimental conditions were optimized before the quantitative analysis of Cu^{2+}. Fig. 2A demonstrated the effect of self–assembly time of capture probe (DNA S1) on the modified electrode surface. With the self–assembly time, the ΔR_{CT} also increased, and reached a plateau at 10 h. Thus, in the subsequent measurements, the self–assembly time of 10 h was used. Similarly, the optimization of hybridization conditions includes hybridization time of DNAzyme hybridization (DNA S2) reaction. The hybridization time is an important factor to ensure the adequacy of a contact reaction. As seen in Fig. 2B, the response current increased sharply with the hybridization time increasing from 30 to 70 min, then leveling off.

The reaction time between DNA with Cu^{2+} would have profound effect on the performance of the biosensor. Upon exposure to 200 nM Cu^{2+}, the ΔR_{CT} increased within 50 min of incubation and then remained constant when there action time was further elongated (Fig. 2C). So, an incubation time of 50 min was employed as the optimum reaction time between DNA with Cu^{2+}. The effect of reaction temperature on the response of the system is also investigated. Fig. 2D depicts the ΔR_{CT} response of the

sensor at varying reaction temperature ranging from 25 to 40 °C. It is observed that the peak current increases with the temperature from 25 to 40 °C and then decreases rapidly as the reaction temperature increases from 40 to 50 °C. Thus 40 °C is chosen as the optimized reaction temperature.

"Here Fig.2"

3.3. Detection of Cu^{2+}

Under the optimized experimental conditions, the modified electrode in 0.1 M PBS (pH 7.4) containing 5 mM $Fe(CN)_6^{3-/4-}$ (1:1) and 10 mM KCl after the electrodes were incubated with different concentrations of Cu^{2+}, and obtained with the Nyquist plots. As seen in Fig. 3A, upon decreasing the concentration of Cu^{2+} from 400 nM to 0.1 nM, less trans-acting catalytic strands cleaved the sessile of the substrate into two fragments, which led to the decrease in ΔR_{CT}. The change in the ΔR_{CT} was linear with the logarithm of the concentration of Cu^{2+} within a concentration range from 0.1 nM to 400 nM. The linear regression equation was $Z= (-602.69\pm28.50)X + (6182.16\pm225.72)$ (Z is the ΔR_{CT} (Ω), X is the common value of the target concentration (M) with a correlation coefficient $r^2=0.9945$. The detection limit (LOD) of this sensor was estimated to be 0.0725 nM (based on S/N=3). As seen in Table 1, this novel impedimetric biosensor showed a comparable LOD and linear detection range compared to other enzyme–based electrochemical DNA sensors for Ag^{+}, Hg^{2+} and Cu^{2+} using EIS, and the linear range and detection limit of this novel electrochemical sensor is comparable to some of the other methods. Moreover, this method is relatively simple.

"Here Fig. 3"

"Here Table 1"

3.4. The reproducibility, stability and selectivity of the biosensor

The reproducibility of this biosensor was investigated. Six biosensors were fabricated with six different GCEs by the same steps independently, and used to detect 200 nM Cu^{2+}, as presented in Fig. 4. The RSD was 4.91% with five biosensors prepared independently, indicating that the fabrication procedure was reliable, and this biosensor had good reproducibility.

The stability of the biosensor was also explored. We investigated the stability of this sensor through the response to 200 nM Cu^{2+} for 1 month (as shown in Fig. S–2B). Beyond this period, the experiment was carried out per 5 days. When not in use, the electrode was stored in a moist state at 4 °C. The result showed that the biosensor retained about 81% of its original ΔI after 1 month. The result indicated that this biosensor has relatively good stability, and the reason might be that the DNAzyme–based sensor is sensitively and specifically responsive to its target ion, and the film (GNCs) could provide a biocompatible microenvironment.

"Here Fig. 4"

Besides, methods related to the sensing of metal ions by the DNAzyme–based sensor concerns the specificity of the system. Thus selectivity of this detection method was tested using impedimetric Cu^{2+} sensor in 0.1 M PBS (pH 7.4) containing 5 mM $Fe(CN)_6^{3-/4-}$ (1:1) and 10 mM KCl. Under the optimal experimental conditions, 200 nM of Cu^{2+}, 2000 nM of Fe^{3+}, Zn^{2+}, Mn^{2+}, Co^{2+}, Hg^{2+}, Pb^{2+}, Cd^{2+} Ca^{2+}, and their mixture containing 200 nM of Cu^{2+}, and their mixture without Cu^{2+} were respectively measured. As seen in Fig. 5, negligible signal response was observed upon the addition of other tested ions, on the contrary, significant response of ΔR_{CT} as observed for Cu^{2+}. Hence, the results showed excellent selectivity toward Cu^{2+} over other ions due to a specificity of DNAzyme for Cu^{2+} ion. Second, Cu^{2+} and other ions were mixed to form a mixture solution as a sample for the anti-jamming capability testing of this sensor (Figure 5). The ΔR_{CT} was obviously higher than other samples without Cu^{2+}. These results clearly indicated that the approach is not only insensitive to other ions but also selective toward Cu^{2+} in their presence. As noted above, the present sensor had excellent selectivity and anti-jamming capability.

"Here Fig. 5"

3.5. Analysis of real samples

To evaluate the practicality of the present method, the biosensor was applied to detect the recoveries of Cu^{2+} with water samples taken from Xiangjiang River, Hunan Province. These Cu^{2+} concentrations in

environmental samples were adjusted to fall in the concentration range from 1 to 200 nM by spiking with Cu^{2+} stock solutions, followed by measuring the Cu^{2+} content using the proposed method and ICP/MS. The results are summarized in Table 2 and show good agreement with those achieved by ICP/MS, indicating that the present sensor can also work in environmental water samples.

"Here Table 2"

4. Conclusions

In summary, a novel impedimetric biosensor was reported to determine Cu^{2+} concentration through use of the difference in charge-transfer resistance (ΔR_{CT}) before and after DNA interactions with Cu^{2+}, ΔR_{CT} is sufficiently sensitive to detect Cu^{2+} as low as 0.0725 nM, and the linear range is from 0.1 M to 400 nM. Moreover, because of the signal amplification on the GNCs platform and the merits of high specificity of the DNAzymes, the sensor maintained high selectivity over other nonspecific metal ions. Considering the good performance of this electrochemical Cu^{2+} sensor, it is expected to obtain great success in environmental monitoring.

ASSOCIATED CONTENT

Supporting Information

More information is detailed about the SEM image of GNCs, Cyclic voltammetry diagrams of GCE, GCE/GNCs, Electrochemical impedance spectra of GCE, GCE/GNCs. This material is available free of charge via the Internet at http://pubs.acs.org.

ACKNOWLEDGMENTS

The authors gratefully acknowledge the Program for Changjiang Scholars (T2011116), the Key Projects of Science and Technology of Hunan Province, China (2012FJ1010 and 2014FJ1011), Natural Science Foundation of China (51474247), National High Technology Research and Development Program of China (2011AA061001) for financial support. Natural Science Foundation of China (51474247).

REFERENCES

1 E.L. Que, D.W. Domaille, C.J. Chang, Chemical Reviews, 2008, **108**, 1517-1549.
2 P.G. Georgopoulos, A. Roy, M.J. Yonone-Lioy, R.E. Opiekun, P.J. Lioy, Journal of Toxicology & Environmental Health Part B Critical Reviews, 2001, **4**, 341-394.

3 A.P.S. Gonzáles, M.A. Firmino, C.S. Nomura, F.R.P. Rocha, P.V. Oliveira, I. Gaubeur, Analytica Chimica Acta, 2009, **636**, 198–204.
4 N.G. Beck, R.P. Franks, K.W. Bruland, Analytica Chimica Acta, 2002, **455**, 11–22.
5 M. Etienne, J. Bessiere, A. Walcarius, Sensors & Actuators B Chemical, 2001, **76**, 531–538.
6 A. Mohadesi, M.A. Taher, Talanta, 2007, **72**, 95–100.
7 B. High, D. Bruce, M.M. Richter, Analytica Chimica Acta, 2001, **449**, 17–22.
8 Q. Suyan, G. Sen, Z. Xi, L. Zhenyu, Q. Bin, C. Guonan, Analyst, 2011, **136**, 1580-1585.
9 Y. Zhou, T. Lin, G. Zeng, J. Chen, J. Wang, C. Fan, G. Yang, Z. Yi, X. Xia, Biosensors & Bioelectronics, 2015, **65**, 382–389.
10 L. Juewen, L. Yi, J.am.chem.soc, 2007, **129**, 9838–9839.
11 Y. Jingjing, L. Jishan, O. Jeremy, Z. Wenwan, Analyst, 2011, **136**, 764-768.
12 Y. Zhang, G.M. Zeng, L. Tang, Y.P. Li, Z.M. Chen, G.H. Huang, Rsc Advances, 2014, **4**, 18485-18492.
13 L. Chen, G. Zeng, Z. Yi, T. Lin, D. Huang, C. Liu, Y. Pang, L. Jie, Analytical Biochemistry, 2010, **407**, 172–179.
14 E.L.S. Wong, P. Erohkin, J.J. Gooding, Electrochemistry Communications, 2004, **6**, 648–654.
15 Z. Peng, B.C. Yin, B.C. Ye, Biosensors & Bioelectronics, 2009, **25**, 935–939.
16 L. Zhang, Y. Zhang, M. Wei, Y. Yi, H. Li, S. Yao, New Journal of Chemistry, 2013, **37**, 1252-1257.
17 G. Chenchen, L. Quan, W. Dou, Z. Shiming, L. Xiaoling, Y. Luxin, X. Xuerong, Z. Lingwen, Analytical Chemistry, 2014, **86**, 6387-6392.
18 X. Miao, L. Ling, D. Cheng, X. Shuai, Analyst, 2013, **137**, 3064-3069.
19 L. Lu, F. Jie, Y. Fan, T. Bo, A. Chem., Analytical Chemistry, 2015, **87**, 4829-4835.
20 Y. Zhou, L. Tang, Xia. X, G. Zeng, J. Wang, Y. Deng, G. Yang, C. Zhang, Y. Zhang, J. Chen, Analyst, 2014, **139**, 6529-6535.
21 R.G. Cao, B. Zhu, J. Li, D. Xu, Electrochemistry Communications, 2009, **11**, 1815–1818.
22 O.A. Cristina, M. Natalia, D.V. Manel, P. Valeri, Analyst, 2013, **138**, 1995-1999.

Table 1 Comparison with other published Cu^{2+} detection sensor and published metal ions detection sensor using EIS.

method	Materials	Linear range ($mol \cdot L^{-1}$)	LOD ($mol \cdot L^{-1}$)	References
Electrochemiluminescence/ DNAzyme	6-carboxyfluorescein	8×10^{-8}–2×10^{-6}	3.5×10^{-9}	10
Fluorescence detection/DNAzyme	Microarray	1×10^{-8}–1×10^{-4}	9.5×10^{-9}	15
Fluorescence detection/DNAzyme	SYBR Green I (SG)	4×10^{-8}–1.2×10^{-6}	1×10^{-8}	16
Colorimetric Detection/DNAzyme	horseradish peroxidise	5×10^{-8}–1.2×10^{-6}	5.9×10^{-9}	17
Colorimetric Detection/DNAzyme	Gold nanoparticles	1×10^{-10}–2×10^{-9}	6×10^{-11}	18
Colorimetric Detection/DNAzyme	Gold Nanoparticle	1×10^{-9}–2×10^{-8}	4.7×10^{-10}	19
Detection Ag^{+}/EIS/DNA	ordered mesoporous carbon nitride material	1×10^{-10}–1×10^{-5}	5×10^{-11}	20
Detection Hg^{2+}/EIS/DNA	Gold electrode	1×10^{-10}–1×10^{-3}	1×10^{-10}	21
Detection Cu^{2+}/EIS/DNAzyme	Avidin–graphite epoxy composite	1×10^{-5}–4×10^{-5}	6.5×10^{-6}	22
Detection Pb^{2+}/EIS /DNAzyme	OMC-GNPs	5×10^{-10} – 5×10^{-5}	2×10^{-10}	9
Detection Cu^{2+}/EIS /DNAzyme	GNCs	1×10^{-10} – 4×10^{-7}	7.25×10^{-11}	This work

Table 2 Determination of Cu^{2+} ions in real samples.

Sample number	Addition concentration (nM)	Biosensor (mean[a] ± SD[b]) (nM)	ICP/MS (mean[a] ± SD[b]) (nM)	Relative Standard Deviation (%)
1	0	12.12±0.89	13.01±0.76	5.00
2	1	20.17±1.3	19.54±1.22	2.24
3	50	71.20±2.4	73.92±1.5	2.65
4	100	113.47±5.1	117.85±6.9	2.68

[a] An average of three replicate measurement. [b]SD =standard deviation

Figure Captions

Fig. 1 Proposed scheme for the illustration of the electrochemical detection of Cu^{2+}.

Fig. 2 Optimization of experimental conditions: (A)effect of self–assembly time (capture probe); (B) effect of hybridization time; (C) the time–course of the Cu^{2+} hybridized with C bases; (D) experiment temperature, upon exposure to 200 M Cu^{2+}. All tested electrodes were fabricated by immobilizing10 μL capture probe on electrodes surfaces at 4 ◦C. Error bars indicate standard deviations from three replicative tests.

Fig. 3 (A) Series of Nyquist plots of the electrode immersed in different concentration of Cu^{2+} (0.1 nM–400 nM). (B) The plot of ΔR_{CT} vs. Cu^{2+} concentration ranging from 0.1 nM–400 nM. Error bars indicate standard deviations from three replicative tests.

Fig. 4 Six different GCEs constructed by the same procedure on response of biosensor for Cu^{2+} (200 nM). Error bars indicate standard deviations from three replicative tests.

Fig. 5 Interference study in the analysis of Cu^{2+} by this biosensor. The data are averages of three replicate measurements. Error bars indicate standard deviations.

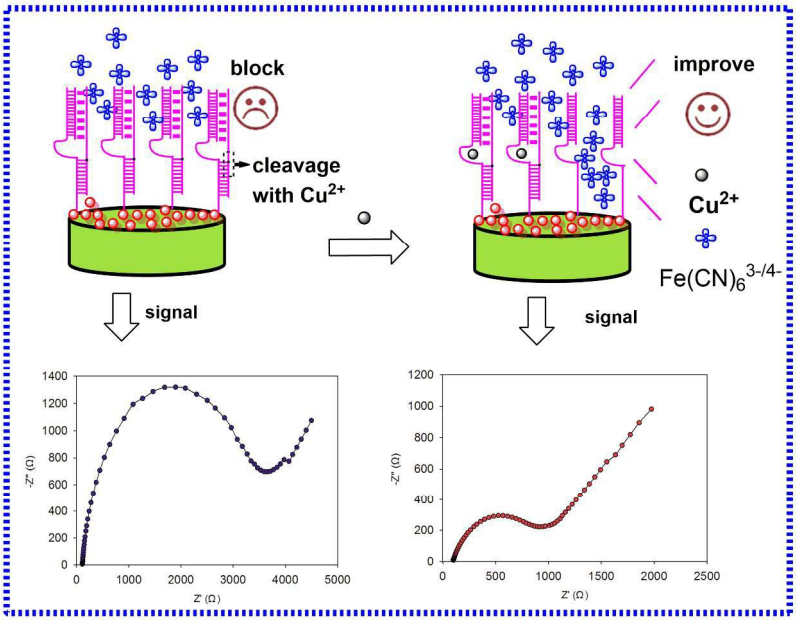

Fig. 1

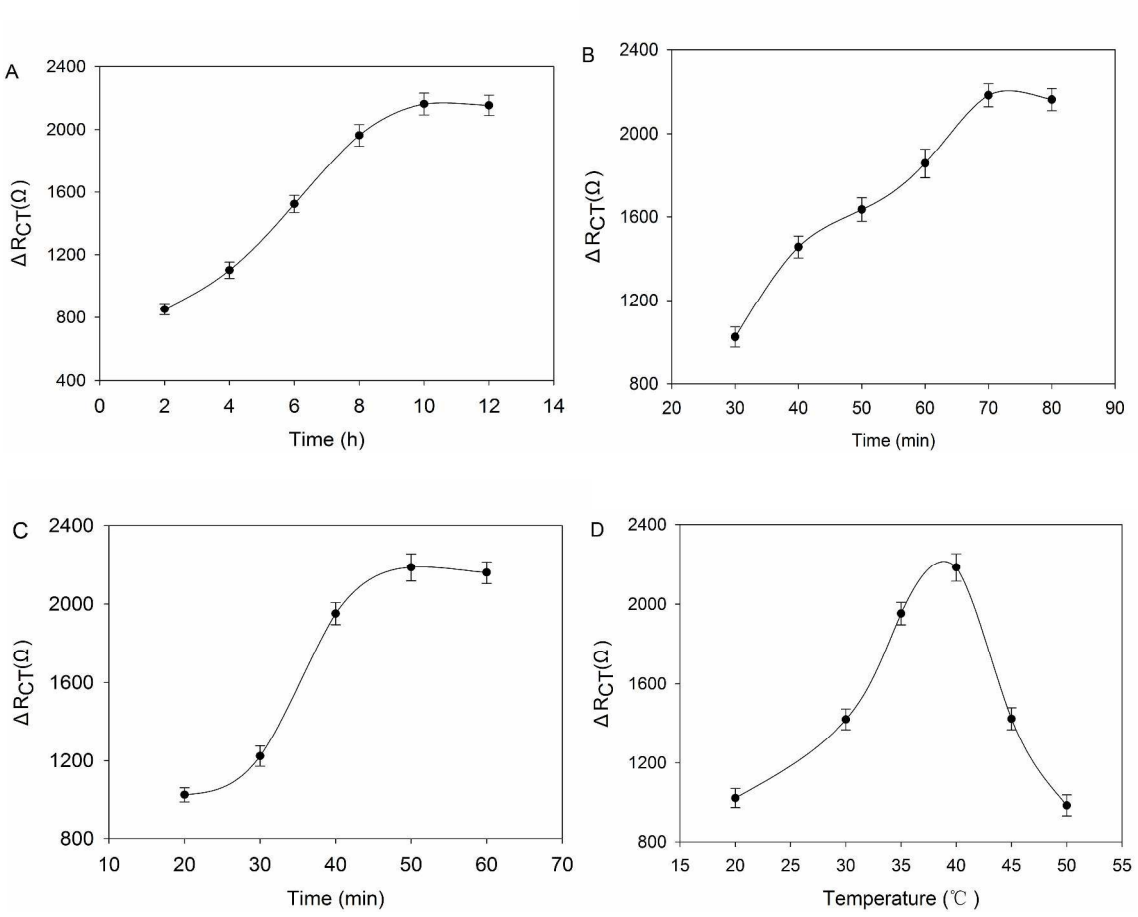

Fig. 2

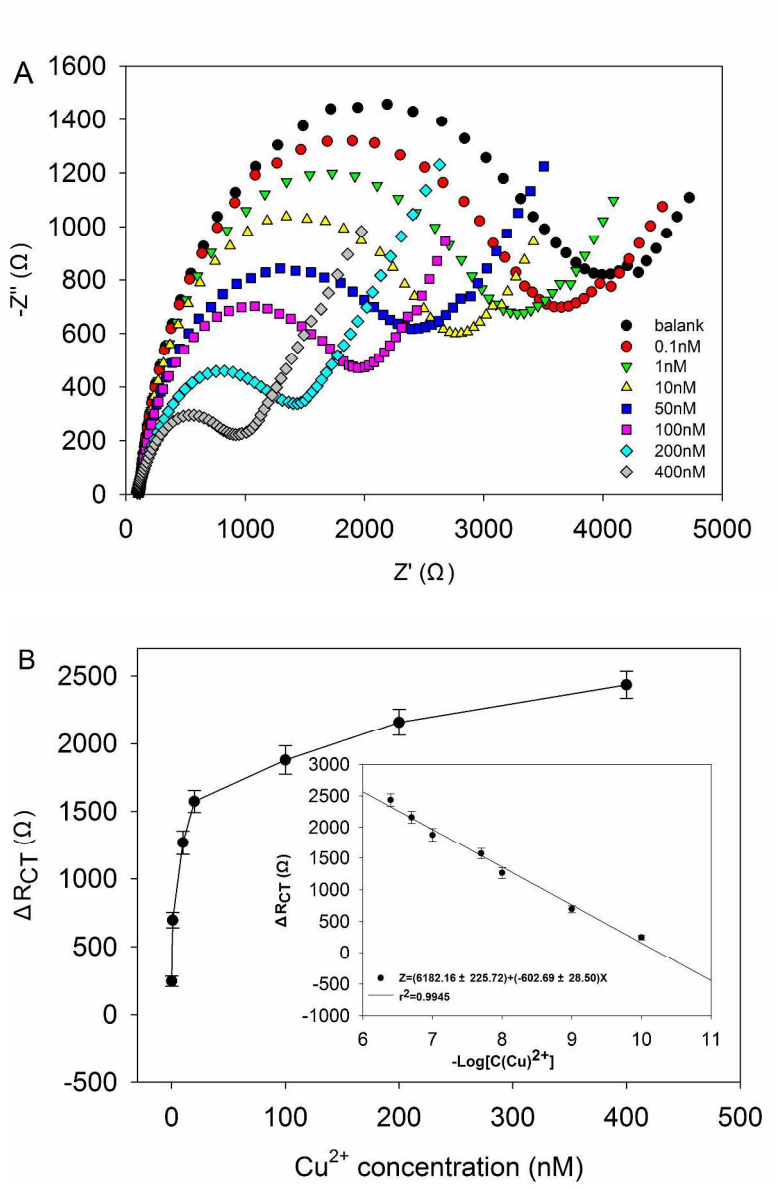

Fig. 3

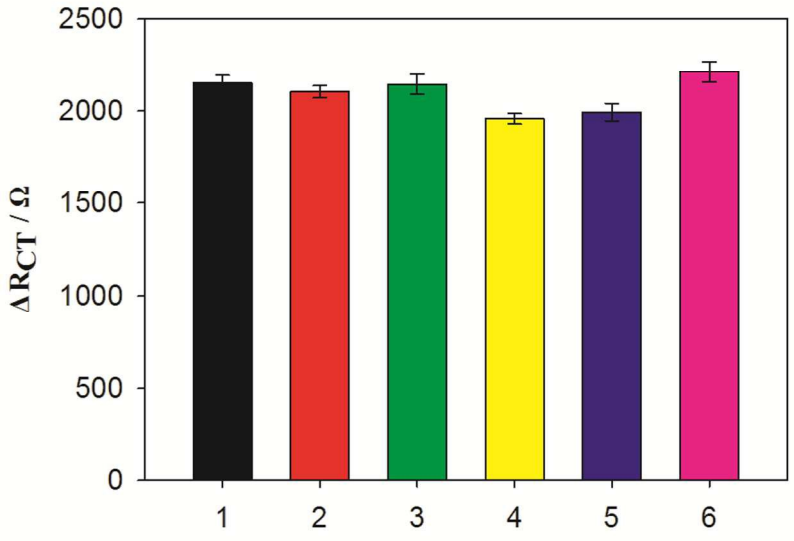

Fig. 4

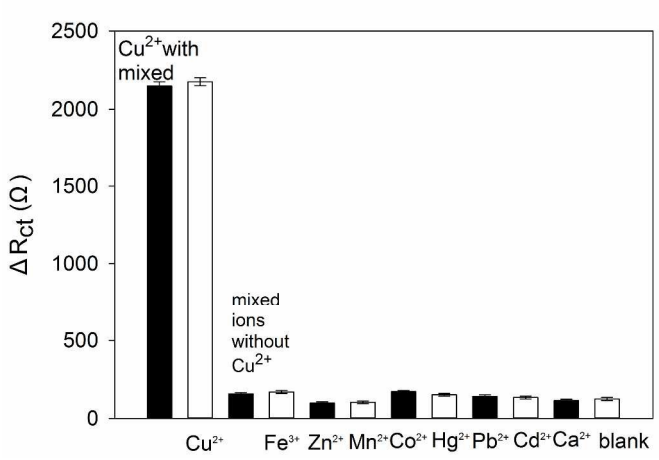

Fig. 5

Graphical Abstract